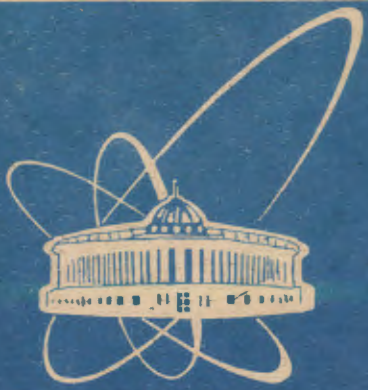

ОБЪЕДИНЕННЫЙ
ИНСТИТУТ
ЯДЕРНЫХ
ИССЛЕДОВАНИЙ

Дубна

96-118

E10-96-118

N.D.Dikoussar*

# FUNCTION PARAMETRIZATION BY USING 4-POINT TRANSFORMS

Submitted to «Computer Physics Communications»

*E-mail address: dikoussar@main1.jinr.dubna.su

1996

# 1 Introduction

The complexity of function approximation problems and main difficulties of the practical implementation of methods for fitting of empiric data are well known and have been studied extensively in recent years [6-13].

This paper is an outcome of further investigations on the new kind of 4-point transformations [1,2], called discrete projective transformations ($\mathcal{DPT}$ or $\mathcal{D}$ - transformations). A new approach based on $\mathcal{DPT}$ is proposed to function parametrization and to approximation of smooth curves on the local segment.

$\mathcal{DPT}$ are new operations (direct and inverse) over the differentiable function defined by a formula or by a table. The $\mathcal{DPT}$ operation has the structure of the "three-point" convolution, using *three* reference points of the curve and *three* weight functions defined by *the cross-ratio* of four collinear points ($CR$–functions). The weight functions are projective invariants, i.e. they are invariable functions with respect to a shift of the basis point and to scaling of their parameters.

New results in function approximation and fitting have been obtained by using four-point transforms. $\mathcal{DPT}$ possess a number of important properties. For example, the direct transform reduces the power of a polynomial by two and is stable to measurement errors everywhere except neighbourhoods of two "*noisy*" points. The inverse transform allows to use coordinates of reference points (the mark $\mathcal{R}$) as continuous parameters of the function: $f(x) = f(x;\mathcal{R})$. Transformation of basis functions $\{x^n\}$ yields the new polynomial basis with the boundary parameters. This basis provides a uniform approximation on the local segment and ensures stability of computations for a vanishing argument. In addition, the system of weight functions has many useful properties [1,2], which allow to design new effective algorithms for data processing.

$\mathcal{DPT}$-approach has a number of advantages with respect to the traditional polynomial approximation. Using $\mathcal{D}$-transforms, the new class of polynomials with a better approximation quality than in $\{x^n\}$ has been derived and a "three-point" model of a cubic spline with the single free parameter is proposed. The model allows to reduce the number of unknown parameters in twice and to obtain an advantage in a computing process.

An additional point to emphasize is that $\mathcal{DPT}$-approach gives a new mathematical tool and a new possibility in both practical applications and theoretical research of computational methods. The application of four-point transforms for fitting of empiric data is simple in practice and provides a wide way for designing adaptive algorithms for digital signal processing, pattern recognition [3], image processing in high-energy physics [4] and so on.

# 2 Definition and properties of transforms

## *2.1 Definition and the geometric sense of $\mathcal{DPT}$*

Four-point transformations were defined in [1,2]. $\mathcal{DPT}$ allow to map points of an arbitrary differentiable curve $f(x)$ (the original) onto corresponding points of another curve $h(\tau)$ (the image) by using three *pivot points* of $f(x)$ and three *weight*

Объединенный институт
ядерных исследований

*functions.* The weight functions are yielded by the cross-ratio of four collinear points: $x$–coordinates of three pivot points $P_0, P_1, P_2$ and of a single variable point $P_f$. Three pivot points of the curve $f(x)$ define the mark of transformations $\mathcal{R}$. The variable point $P_f$ is mapped into the point $P_h$

$$\mathcal{D} : P_f \longmapsto P_h, \tag{1}$$

where $P_f \equiv P_f(x, f(x))$, $P_h \equiv P_h(\tau, h(\tau))$, and $\tau = x - x_0$.

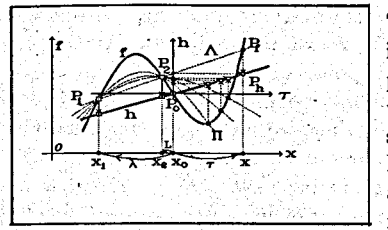


The ordinate of $P_h$ is defined as the point of intersection of *the parabola* or *the straight line* passing through three points ($P_1, P_2$ and $P_f$) with axis $\tau = 0$ ($x = x_0$) (fig.1). The basis point $P_0$ remains as *the immovable point.* Pivot points $P_1$ and $P_2$ are transformed by an approximate limit, when $x \to x_1$ and $x \to x_2$, respectively (see subsection 2.3).

Fig.1. The scetch of the geometric sense of $\mathcal{DPT}$.

Let us denote $\lambda = x_1 - x_0, L = x_2 - x_0$, $f_\lambda \equiv f(x_0 + \lambda)$ and $f_L \equiv f(x_0 + L)$. Values $\lambda$, $L$ are parameters and $\mathcal{R} : \{P_0(x_0, f_0), P_1(x_0 + \lambda, f_\lambda), P_2(x_0 + L, f_L)\}$ is a mark of the transformations.

It is seen from the definition that the 4-point transformations depend on their parameters and on the mark, i.e. the shape and the position of the image-curve $h(\tau)$ are determined on a plane not only by the function $f(x)$, but also by the choice of the mark $\mathcal{R}$.

In what follows the direct and inverse transformations will be denoted as

$$f^{\triangleleft}(x; \mathcal{R}) \equiv \mathcal{D}[f(x); \mathcal{R}] = h(\tau) \tag{2}$$

and

$$h^{\triangleright}(\tau; \mathcal{R}) \equiv \mathcal{D}^{-1}[h(\tau); \mathcal{R}] = f(x). \tag{3}$$

These operations have the visual geometric sense (see fig.1). The image-curve $h = f^{\triangleleft}(x; \mathcal{R})$ is the geometric locus of points of intersection of the parabola $\Pi$ or the straight line $\Lambda$, passing through three points $P_1, P_2$ and $P_f$ with the basis axis $\tau = 0$. In case of the inverse transformation, the ordinate $h(\tau)$ is taken on the basis axis and the point of intersection is taken on the perpendicular $\tau = x - x_0$.

To express $\mathcal{DPT}$ in the analytical form, we use the scalar product for 3D vectors $\vec{P}, \vec{F}, \vec{D}$ and $\vec{Z}$:

$$f^{\triangleleft}(x; \mathcal{R}) = (\vec{P}, \vec{F}) = \sum_{i=1}^{3} p_i(\tau; \lambda, L) f_i \tag{4}$$

and

$$h^{\triangleright}(\tau; \mathcal{R}) = (\vec{D}, \vec{Z}) = \sum_{i=1}^{3} d_i(\tau; \lambda, L) z_i, \tag{5}$$



where $\vec{P} = (p_1, p_2, p_3)^T, \vec{D} = (d_1, d_2, d_3)^T, \vec{F} = (f_\lambda, f_L, f(x))^T, \vec{Z} = (f_\lambda, f_L, h(\tau))^T$. Functions $p_i(\tau; \lambda, L)$ and $d_i(\tau; \lambda, L)$ are $CR$ or *weight functions* (see table 1).

### *2.2 CR-functions and their properties*

Unlike the classical cross-ratio algorithm [5] of 4 collinear points $(x_1, x_2, x_3, x_4)$ (fig.2), we use the algorithm with the rearrangement the position of two points [1,2] as the following:

$$\frac{\Delta_{13}}{\Delta_{24}} : \frac{\Delta_{23}}{\Delta_{14}}, \tag{6}$$

where $\Delta_{ij}$ denotes the algebraic distance between points $i$ and $j$, i.e. $\Delta_{ij} = x_j - x_i$. For the single fixed point the cross-ratio (6) yields only three various functions defined by the position of points in the quadruple on the number axis (fig.2).

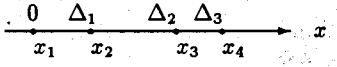


Fig.2.

For example, if $x_1$ is the fixed point and $\Delta_j = x_{j+1} - x_1$, $(j = 1, 2, 3)$, then distances $\Delta_{ij}$ can be expressed through $\Delta_j$:

$$\Delta_{13} = \Delta_2, \ \Delta_{14} = \Delta_3, \ \Delta_{23} = \Delta_2 - \Delta_1 \text{ and } \Delta_{24} = \Delta_3 - \Delta_1.$$

Substituting $\Delta_{ij}$ in (6) and using index point functions $m(i)$ and $n(i)$, $CR$-functions $p_i(\Delta_1, \Delta_2, \Delta_3)$ are written as the following:

$$p_i(\bar{\Delta}) = \frac{\Delta_m \Delta_n}{(\Delta_i - \Delta_m)(\Delta_i - \Delta_n)}, \ i = 1, 2, 3, \tag{7}$$

where $m = m(i) = 2 - i + (i - 1)!$, $n = n(i) = 4 - (i - 1)!$, and $\bar{\Delta} = (\Delta_1, \Delta_2, \Delta_3)$. From the above and eq.(7) it follows that $CR$–functions are dimensionless, scaling-invariant and translation-invariant functions:

$$p_i(\mu\bar{\Delta}) = p_i(\bar{\Delta}), \ d_i(\mu\bar{\Delta}) = d_i(\bar{\Delta}), \ \mu \neq 0, \ i = 1 \div 3.$$

If we denote $\Delta_j = \lambda, L, \tau$, for $j = 1, 2, 3$ respectively, then functions $p_i(\bar{\Delta})$ and $d_i(\bar{\Delta})$ are written for the quadruplet $\{0, \lambda, L, \tau\}$ by formulae in table 1. The important property of $p_i$ and $d_i$ is the natural normalization of their sums:

$$\sum_{i=1}^{3} p_i(\tau; \lambda, L) = 1 \tag{8}$$

and

$$\sum_{i=1}^{3} d_i(\tau; \lambda, L) = 1. \tag{9}$$

To proof these equalities, we can use an ordinary summation of corresponding functions from table 1. Main characteristics of weight functions and their graphs for fixed $\lambda$ and $L$ are indicated in table 1 and in fig.3.

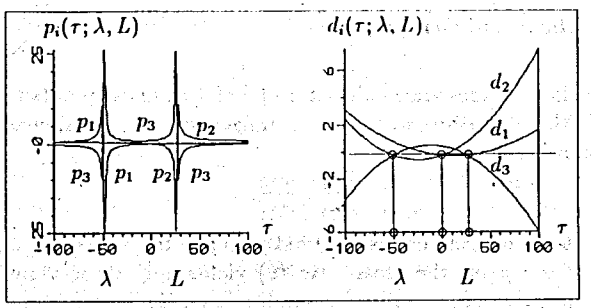


Fig.3. Graphs of $p_i$ and $d_i$ functions (fragments).

To find the inverse transform functions $d_i(\bar{\Delta}), i = 1,2,3$, we divide both parts of the equality (8) by $p_3 \neq 0$:

$$d_1 = -\frac{p_1}{p_3},\ d_2 = -\frac{p_2}{p_3},\ d_3 = \frac{1}{p_3}.$$

*The system of three functions* $\{p_i(\tau;\lambda,L)\}, i = 1,2,3$ has *the threefold symmetry* and possesses a number of useful properties considered in ref. [1,2]. For example, functions $p_1$ and $p_2$ are obtained from $p_3$ by the formal rearrangement of parameters and the variable: $\lambda \rightleftharpoons \tau$ and $L \rightleftharpoons \tau$ respectively. This symmetry is shown in the form of the diagram for calculation of $p_i$ (fig.4). Here, the structure of the system is represented under condition as three overlapping triangles.

Table 1. $CR$–functions and their characteristics.

| $CR-f$ | formulae | zeros | $\tau_e$ | extremum | h/asympt. | v/asympt. |
|---|---|---|---|---|---|---|
| $p_1$ | $\frac{L\tau}{(\tau-\lambda)(L-\lambda)}$ | 0 | no | no | $p_1 = \frac{L}{L-\lambda}$ | $\tau = \lambda$ |
| $p_2$ | $\frac{-\lambda\tau}{(\tau-L)(L-\lambda)}$ | 0 | no | no | $p_2 = \frac{-\lambda}{L-\lambda}$ | $\tau = L$ |
| $p_3$ | $\frac{\lambda L}{(\tau-\lambda)(\tau-L)}$ | no | $\frac{L+\lambda}{2}$ | $\frac{-4\lambda L}{(L-\lambda)^2}$ | $p_3 = 0$ | $\tau = \lambda, L$ |
| $d_1$ | $\frac{-\tau(\tau-L)}{\lambda(L-\lambda)}$ | $0, L$ | $\frac{L}{2}$ | $\frac{-L^2}{4\lambda(L-\lambda)}$ | no | no |
| $d_2$ | $\frac{\tau(\tau-\lambda)}{L(L-\lambda)}$ | $0, \lambda$ | $\frac{\lambda}{2}$ | $\frac{\lambda^2}{4L(L-\lambda)}$ | no | no |
| $d_3$ | $\frac{(\tau-\lambda)(\tau-L)}{\lambda L}$ | $\lambda, L$ | $\frac{L+\lambda}{2}$ | $\frac{-(L-\lambda)^2}{4\lambda L}$ | no | no |



We see, that functions $p_i(\tau;\lambda,L)$ are calculated by division of quantities in the isolated vertex of the triangle into the product of differences, which disposed in the other corners.

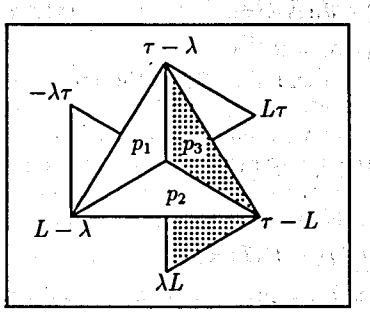


Fig.4. The diagram for computing of $p_i(\tau;\lambda,L)$.

As indicated on the diagram, 12 operations are needed for calculation of all three functions at the single variable point. Six operations of the first level are disposed at vertices of triangles. On the second level we have 3 multiplications of pairwised differences. Three divisions are fulfilled on the third level of calculation. If these calculations are carried out for every level in a parallel way, then all three functions can be calculated in the time of fulfilling of three operations: $-$, $\times$ and $\div$.

*2.3 The dpT algorithm*

Equations (4), (5) and formulae from table 1 define the transformation rule for all curve points except of two pivot points, where functions $p_i$ have endless discontinuities. The basis point is the fixed point: $h(x_0) = f(x_0)$. One can find the values $h(\cdot)$ at pivot points by the substitution of $p_i$ in (4). Taking into account (8) for $\tau = x - x_0, \lambda = x_\lambda - x_0, L = x_L - x_0$ and $x_0 = 0$, we find:

$$h(\tau) = \sum_{i=1}^{3} p_i f_i = -\frac{L\tau}{L-\lambda}\cdot\frac{f(\tau)-f(\lambda)}{\tau-\lambda} + \frac{\lambda\tau}{L-\lambda}\cdot\frac{f(\tau)-f(L)}{\tau-L} + f(\tau).$$

Hence, on the strength of differentiability $f(\tau)$ under $\tau \to \lambda$ and $\tau \to L$, we find $h(\lambda)$ and $h(L)$:

$$h(\lambda) = \lim_{\tau\to\lambda} h(\tau) = -\frac{\lambda L}{H}f'(\lambda) + \frac{\lambda^2}{H^2}\Delta f_{L\lambda} + f(\lambda) \qquad (10)$$

and

$$h(L) = \lim_{\tau\to L} h(\tau) = \frac{\lambda L}{H}f'(L) - \frac{L^2}{H^2}\Delta f_{L\lambda} + f(L), \qquad (11)$$

where $H = L - \lambda, \Delta f_{L\lambda} = f(L) - f(\lambda)$, and if $x_0 \neq 0$, parameters $\lambda$ and $L$ are replaced by $x_0 + \lambda$ and $x_0 + L$ for $f(\cdot)$ and $f'(\cdot)$ respectively.

Formulae from table 1 and eqs.(4), (5), (10), (11) are basic formulae of the $dpT$-algorithm for calculation direct and inverse transforms of the smooth function, given by the formula or by the table:

$$h(\lambda) = -\frac{\lambda L}{H}f'(x_\lambda) + \frac{\lambda^2}{H^2}(f_L - f_\lambda) + f_\lambda,$$

$$h(L) = \frac{\lambda L}{H}f'(x_L) - \frac{L^2}{H^2}(f_L - f_\lambda) + f_L,$$

$$h(\tau) = p_1(\bar{\Delta})f_\lambda + p_2(\bar{\Delta})f_L + p_3(\bar{\Delta})f(x),$$

$$h(0) = f(x_0), \tau = x - x_0,\ H = L - \lambda, \tag{12}$$

and

$$f(x) = d_1(\bar{\Delta})f_\lambda + d_2(\bar{\Delta})f_L + d_3(\bar{\Delta})h(\tau), \tag{12a}$$

where $\lambda = x_\lambda - x_0, L = x_L - x_0$, and $\bar{\Delta} = (\tau; \lambda, L)$.

To obtain relation between the derivative $f'(\cdot)$ and $f^q(\cdot; \mathcal{R})$ at the reference points, we use eqs.(10) and (11):

$$f'(x_0 + \lambda) = \frac{1}{\lambda L H}[\lambda^2 \Delta f_{L\lambda} + H^2(f_\lambda - f^q(\lambda; \mathcal{R}))] \tag{13}$$

and

$$f'(x_0 + L) = \frac{1}{\lambda L H}[L^2 \Delta f_{L\lambda} - H^2(f_L - f^q(L; \mathcal{R}))]. \tag{14}$$

*Remark 1.* The *dpT* algorithm gives the rule for realization of two reciprocal operations over the smooth curve $f(x)$ for the given mark $\mathcal{R}$. The outcome of the operation is the new function (the image), complexity of which differ by two orders from the initial function (the original). Subtracting $f(x_0)$ from both parts of eq. (12) for $h(\tau)$, we find:

$$f^q(x; \mathcal{R}) = f_0 + \sum_{i=1}^{3} \Delta f_i p_i(\bar{\Delta}),\ \text{where } \Delta f_i = f_i - f_0.$$

This formula expresses the relation between function increments $\Delta f_i$ and argument increments $\Delta x_i$, defined by coordinates of three points $P_1, P_2, P_f$ with respect to the point $P_0$ and by using *the cross-ratio* of $x-$ coordinates of these points. (The relation between $\Delta f$ and $\Delta x$ in case of the derivative is established by the existence limit when $\Delta x \to 0$ for *the simple ratio* of increments with respect to $P_0$. The geometric sense of the derivative is defined by the parameters of the tangent in $P_0$). From the geometric point of view, the curve $f^q(x; \mathcal{R})$ is defined by the position and by the shape (the slope) of the parabola (the straight line) passing through three points onto "the body" of the curve (fig.1). Thus, we can assume the operation $f^q(x; \mathcal{R})$ as it was *"the projective derivative"* of the function for the given mark $\mathcal{R}$ defined by three reference points $P_0, P_1$ and $P_2$ on the original curve.

### *2.4 The relation between CR and LQ functions*

The family of linear and quadratic ($LQ$) functions $y(x) = ax^2 + bx + c$, ($a, b, c-$ real numbers) has particular interest from the viewpoint of $\mathcal{DPT}$. In this case vectors $\vec{F}$ and $\vec{Z}$ for every term (to within multiplier) have the following form:

$$\vec{Y} = (\lambda^k, L^k, x^k)^T, \vec{Z} = (\lambda^k, L^k, x_0^k)^T, k = 0, 1, 2.$$

Shifting the origin of coordinates at the point $\mathcal{P}_0(x_0, y_0)$ and substituting $p_i$ and $\vec{Y}$ in (4), we obtain $h = 0$, i.e. $\vec{P}$ and $\vec{Y}$ are *orthogonal* vectors.

$$(\vec{P}, \vec{Y}) = 0. \tag{15}$$

The property (15) affects the projective nature of $\mathcal{DPT}$ and plays the important role in their structure. Eq.(15) establishes the coupling between projective



invariants (7) and four points of the $LQ-$function $\{y_j = ax_j^2 + bx_j\}, j = 0 \div 3$ on an Euclidean plane. In particular, eq.(15) yields the error equation in transforming the $LQ-$function given by experimental points:

$$(\vec{P}, \vec{Y} + \vec{E}) = (\vec{P}, \vec{Y}) + (\vec{P}, \vec{E}) = 0 + \epsilon, \tag{16}$$

where $\vec{E} = (e_\lambda, e_L, e_\tau)^T$ is the error vector, and $\epsilon$ is the total error of the transformation. Hence, if random errors have the $LQ-$dependence at the 4-point system, then the error $\epsilon$ becomes zero at the transformation point.

If we denote $e_{max} = max\{\mid e_\lambda \mid, \mid e_L \mid, \mid e(\tau) \mid\}$, then the transformation error $\epsilon_h(\tau)$ can be estimated by the following inequality:

$$\epsilon_h(\tau) \le U e_{max}, \tag{17}$$

where

$$U(\tau; \lambda, L) = \sum_{i=1}^{3} \mid p_i(\tau; \lambda, L) \mid .$$

In particular, taking into account horizontal asymtotes of $p_i$ (table 1), the function $U \to \frac{|L|+|\lambda|}{|L-\lambda|}$ in $\tau \to \infty$ and if $\lambda L < 0$, then $U \to 1$, i.e. the transformation error is not greater than $e_{max}$.

The example of the graph of the function $U(\tau; \lambda, L)$ for fixed $\lambda = -50, L = 25$ and $x_0 = 0$ is shown on fig.5. "Noisy" ($U(\tau; -50, 25) > 1$) zones are shown on the scale under axis $\tau$. The example of the noise transfer $n(x) \sim \mathcal{N}(0, \sigma)$ in transforming of the five order polynomial $\tilde{M}_5(x) = -(x^5 - 5x^3 + 4x) + n(x)$ ($x_0 = 0, \lambda = -1$ and $L = 2$) is shown in the right part of fig.5. The result of the transformation is the noised cubic curve $\tilde{h}(x) = 2(x^3 + x^2 - 2x) + n^q(x)$, which has " rejections" in neighborhoods of $\lambda$ and $L$.

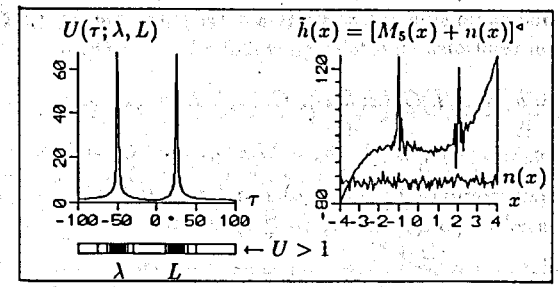


Fig.5. The graph of $U(\tau; 50, 25)$ and the effect of the noise transformation.

It follows from (15) - (17) that the operation $f^q(x; \mathcal{R})$ suppresses the error almost everywhere with the exception of neighborhoods of "noisy" points $\lambda$ and $L$. This property of $\mathcal{DPT}$ plays the important role and can be very useful in data processing. As we known, the derivative and the difference scheme are highly unstable in this case even to small measurement errors.

The above formalism is the useful means for function parametrization. The use of $\mathcal{DPT}$ for obtaining the special class of polynomials (monosplines) with the good approximation quality is considered in the next section.

# 3 The transform of $\{x^n\}$

*3.1 Basic function parametrization (the direct transform)*

Power functions (or monomials) $\{x^n\}, n = 0,1,2,\cdots$ play the important role in the calculus first of all as the linearly independent basis for the power-series expansion of main elementary functions. The class of power functions has the special interest from point of view of our transforms.

The formula for $\mathcal{D}[x^n;\mathcal{R}_n]$ in $x_0 = 0$ and $\vec{F}_n \doteq [\lambda^n, L^n, x^n]^T$ was derived in ref.[1]:

$$h_n = [x^n;\mathcal{R}_n]^q = \lambda L x \sum_{i=1}^{n-1} \lambda^{i-1} \sum_{k=1}^{n-i-1} L^{k-1} x^{n-i-k-1} = \lambda L x G_n(x;\lambda,L), \qquad (18)$$

where $n = 0,1,2,\cdots$, $G_n(x;\lambda,L)$ are elementary symmetric functions and $\mathcal{R}_n$ is the mark for $x^n$

$$\mathcal{R}_n : \{\mathcal{P}_0, \mathcal{P}_\lambda^n, \mathcal{P}_L^n\},\ (\lambda, L \neq 0;\ \lambda \neq L),\ \mathcal{P}_j^n = \mathcal{P}_j(j, j^n), j = 0, \lambda, L. \qquad (19)$$

It follows from (18) that $h_n$ are homogeneity functions with respect to $\lambda, L, x$ of the power $n$ and $n-2$ power functions relative to $x$. So, in general, the operation $M^q(\cdot)$ decreases the polynomial power by two:

$$[M_n(x);\mathcal{R}]^q \doteq M_{n-2}(x;\lambda,L),$$

where $M_{n-2}(x;\lambda,L)$ is the $n-2$ power polynomial depending on $x$. In particular, the straight line and quadratic parabola are mapped into a constant, the cubic parabola into a straight line and so on ($G_0 = G_1 = G_2 = 0$). Eq.(18) can be noted also as recursion relations:

$$h_n(x;\lambda,L) = h_3(x;\lambda,L)G_n(x;\lambda,L),\ G_n(x;\lambda,L) = g_n(x;L) + \lambda G_{n-1}(x;\lambda,L),$$

$$g_n(x;L) = x g_{n-1}(x;L) + L^{n-3},\ \ h_3 = \lambda L x,\ g_3 = 1,\ G_3 = 1,\ n = 4,5,\cdots. \qquad (20)$$

Thus, the polynomial $M_{n-2}(x;\lambda,L)$ can be represented as a product of the polynomial related to $\{G_n(x;\lambda,L)\}$, $(n \geq 3)$ and the function $h_3 = \lambda L x$, i.e.

$$\mathcal{D}[M_n;\mathcal{R}] = \sum_{j=0}^{n} a_j [x^j;\mathcal{R}_n]^q = a_0 + \lambda L x \sum_{j=3}^{n} a_j G_j(x;\lambda,L),$$

where $\{G_n(x;\lambda,L)\}$ is the continuously parameterized basis by parameters $\lambda$ and $L$. For the symmetric choice of parameters ($\lambda = -L$) functions $G_n(x;\lambda)$ depend on the single parameter $\lambda$ and have a more simple form:

$$G_n(x;\lambda) = x G_{n-1}(x;\lambda) + \frac{(-1)^{n-3}+1}{2}\lambda^{n-3},\ n = 3,4,\cdots,\ G_1 = G_2 = 0. \qquad (21)$$

Formulae for $G_n(x;\lambda,L)$, $n = 3,4,...,8$ are given in table 2.



Table 2.

| $n$ | $G_n(x;\lambda,L)$ | $G_n(x;\lambda)$ |
|---|---|---|
| 3 | 1 | 1 |
| 4 | $(x+L)+\lambda G_3$ | $x$ |
| 5 | $x(x+L)+L^2+\lambda G_4$ | $x^2+\lambda^2$ |
| 6 | $x(x(x+L)+L^2)+L^3+\lambda G_5$ | $x^3+x\lambda^2$ |
| 7 | $x(x(x(x+L)+L^2)+L^3)+L^4+\lambda G_6$ | $x^4+x^2\lambda^2+\lambda^4$ |
| 8 | $x(x(x(x(x+L)+L^2)+L^3)+L^4)+L^5+\lambda G_7$ | $x^5+x^3\lambda^2+x\lambda^4$ |

*3.2 Basic function parametrization (the inverse transform)*

Let us consider functions $\{x^n\}, n = 0,1,2,...$ and their representations by using the inverse $\mathcal{D}PT$. Using marks $\mathcal{R}_n$ (19) and eq.(5), we obtain

$$x^n = \lambda^n d_1 + L^n d_2 + h_n(x;\lambda,L)d_3,\ n = 0,1,2,....$$

We shall denote the third term by $S_n(x;\lambda,L)$ and after substitution of $h_n$ from (18) and $d_3(x;\lambda,L)$ into the above expression we obtain:

$$S_n(x;\lambda,L) = x(x-\lambda)(x-L)G_n(x;\lambda,L),\ n = 3,4,5,.... \qquad (22)$$

Eqs. (22) define the class of the functions, having zeros $\lambda$, $L$ and 0. From here, we have for $S_n(\lambda) = S_n(L) = 0$:

$$[S_n;\mathcal{R}_n]^q = 0p_1 + 0p_2 + S_n p_3 = \lambda L x G_n(x;\lambda,L) = h_n = [x^n;\mathcal{R}_n]^q,$$

i.e. $\mathcal{D}-$ transformations of $S_n$ and of $x^n$ coincide. The connection between $S_n(x;\lambda,L)$ and $x^n$ are given by the following relation:

$$S_n(x;\lambda,L) = x^n - \lambda^n d_1 - L^n d_2 = x^n + (-1)^n \frac{\lambda^{n-1}}{H}x(x-L) - \frac{L^{n-1}}{H}x(x-\lambda), \qquad (23)$$

$n = 3,4,5,...$, where $H = L - \lambda$, and $d_1$, $d_2$ are taken from table 1. The equation (23) for the symmetric case has the simpler expression:

$$S_n(x;\lambda) = x^n - \lambda^{n-m}x^m,\ m = 1 + \frac{(-1)^n+1}{2},\ n = 3,4,5,.... \qquad (23a)$$

Fig.6 shows fragments of graphs of such functions in the form of surfaces $S_n(x;\lambda)$ $(x,\lambda \in [-1,1])$. Graphs of $S_n(x;1)$ for $n = 3,4,5,6$ are shown on fig.7.

Polynomials $S_n(x;\lambda,L)$ have the structure of *nth* order *monosplines*, which play, in the known sense, the same role in the approximation theory as Chebyshev polynomials do in the classical function approximation theory [9]. From geometric point of view, functions $S_n(x;\lambda,L)$ are obtained by means of the algebraic summation of the monomial $x^n$ with the $LQ-$function, depending on the value and the

parity of the number $n$ and on pivot coordinates $\lambda, L$.

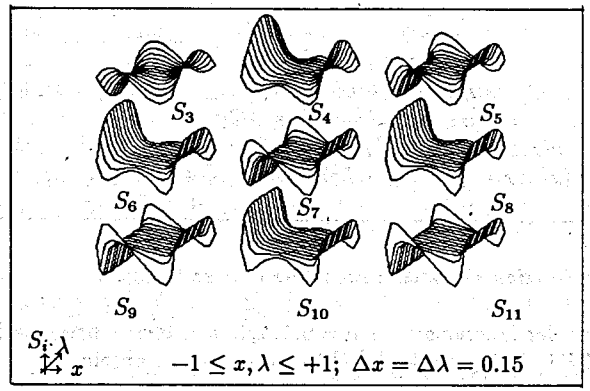


Fig. 6. Surfaces $S_n(x;\lambda)$ for $x, \lambda \in [-1,1]$.

The behaviour of $S_n(x;\lambda,L)$ has the quality difference from the behaviour of $x^n$ for vanishing $x$. It is well known, the polynomial model, based on $\{x^n\}$ leads to ill-conditioned matrices and to the round-off error accumulation in solving a number of statistic tasks for the large dimension $n$ and the large sample in vanishing $x$. Functions $\{S_n(x;\lambda,L)\}$ do not suffer so from similar situations, since they have *the damping terms*, which provide the computing stability. The position of the roots on the plain should be taken into consideration. Comparing with $x^n$ roots, we see that the polynomial $S_n(x;\lambda,L)$ has roots $0, \lambda, L$ and roots of the equation $G_n(x;\lambda,L) = 0$, which, in generally, are complex-valued.

Using $\mathcal{DPT}$ (12a) in $x_0 = 0$, the arbitrary function $f(x) \in C[a,b]$ can be decomposed in the following way:

$$f(x) \equiv f(x;\mathcal{R}) = f(\lambda)d_1(x;\lambda,L) + f(L)d_2(x;\lambda,L) + f^q(x;\mathcal{R})d_3(x;\lambda,L). \quad (24)$$

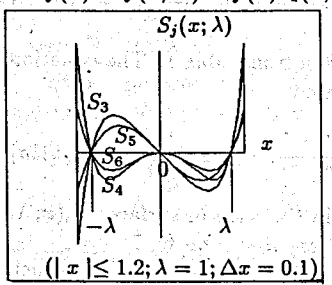


Fig.7. Graphs of $S_j(x;1)$.

So, in general, if we have three reference points on the curve $f(x) \in C[a,b]$ and the image-function $h(x;\lambda,L) \equiv f^q(x;\mathcal{R})$ is known, then we can offer the function $f(x)$ in the parameterized form (24). The formula (24) is very useful in processing of the curve given by a table or by experimental points $\{\tilde{f}_k\}$ because of $\tilde{f}_k^q(x;\mathcal{R})$ can be calculated through measurement points.

Eq. (18) and decomposition (24) allow to change the behaviour of the error in local function approximation by the modified truncated power-series. For example, using (24) five terms of the Taylor-series for $f(x) = e^x, x \in [-\lambda,\lambda]$ and $G_n(x;\lambda)$



from table 2, we obtain:

$$e^x \approx \varphi(x;\lambda) = e^{-\lambda}d_1 + e^{\lambda}d_2 + [\sum_{k=0}^{5}\frac{x^k}{k!};\lambda]^q d_3 = \frac{1}{2\lambda^2}x[e^{-\lambda}(x-\lambda) + e^{\lambda}(x+\lambda)]$$
$$-[1+0+0-\lambda^2 x(\frac{1}{6}+\frac{x}{24}+\frac{(x^2+\lambda^2)}{120})]\frac{(x^2-\lambda^2)}{\lambda^2}.$$

This notion in $\lambda = 1$ gives the residual $r = \mid e^x - \varphi(x) \mid < .0007$, $x \in [-1,1]$ with zeros at boundary points, whereas the result for the original series with the same conditions makes up $r < .00153$, mainly on interval borders. The error in the central part of the segment for the original series is less than for the transformed series. We see that this simple and clear way leads to *the error redistribution* on the segment. The above example shows that $\mathcal{DPT}$ and polynomials $G_n(x;\lambda,L)$ provide a useful tool to operate with truncated power-series.

Eq.(24) has a number of advantages in solving local approximation tasks at least in two aspects: a) the number of unknown parameters in (24) is smaller by two, than in presentation of $f(x)$ by the traditional polynomial; b) when the function is given by the array of measurements $\{\tilde{f}_k\}, k = 1,2,...$, the choice of pivot points allows many variations, that are the source of the flexibility in the practical use of the method, especially for pattern recognition and for adaptive digital signal processing.

On the other hand, formulae (12), (23), and (23a) allow to derive the approximation of the smooth single-valued function $f(x)$ trough functions $d_1(x;\lambda,L)$, $d_2(x;\lambda,L)$ and the parameterized basis $\{S_n(x;\lambda,L)\}, n = 3,4,\cdots$, yielding by $\mathcal{DPT}$ of the basis $\{x^n\}$ for marks (19).

For example, if the function $f^q(x;\mathcal{R})$ is unknown, then taking parameters $\lambda$ and $L$ as boundaries of the interval, assuming $f^q(x;\mathcal{R})) \approx \sum_k \alpha_k G_k(x;\lambda,L)$, and using (24), we obtain the expansion of $f(x)$ on $[\lambda,L]$ by polynomials $d_1$, $d_2$ and $\{S_n\}, n = 3,4,\cdots$ with unknown coefficients $\alpha_k = \alpha_k(\mathcal{R}_k)$:

$$f(x) \approx f(x;\mathcal{R}) = \Pi + S_3(x;\lambda,L)\sum_{k=3}^{n}\alpha_k G_k(x;\lambda,L) = \Pi + \sum_{k=3}^{n}\alpha_k S_k(x;\lambda,L), \quad (25)$$

where $\Pi = \Pi(x;\lambda,L) = f_0 + f(x_\lambda)d_1(x;\lambda,L) + f(x_L)d_2(x;\lambda,L)$.

As mentioned above, the transformation of basis functions $\{x^n\}$, properties of $\mathcal{DPT}$ and formulae (12) - (14), (20), (23) - (25) should be utilized for solving the wide class of the practical problems, which use function approximation and data fitting. This approach can be fruitful for processing both analytical and tabulated functions. The conception of "three pivot points on the curve" yields the new possibility for designing adaptive algorithms for finding and recognizing of curves of a complex shape with errors and backgrounds.

# 4 Function approximation and fitting

In this section we consider some applications of $\mathcal{DPT}$ and $\{S_n(x;\lambda,L)\}$ for function approximation, interpolation and fitting.

It is known [6,7], the traditional polynomials have a number of disadvantages, appearing in interpolation of the functions which have the peculiarity of the behaviour in a local zone. O. Runge function is the example of such a situation [6]. Recently, spline methods enjoy a wide application for function approximation [8-10]. The splines devoid of this lack and being by the efficient tool both in theoretical research and in applications. Many papers concerned with function interpolation and approximation are appeared up to now [12,13]. The cubic model of Hermite spline $S(f;x)$ has become most frequent in practice. Let us consider this model in the analytical form [9]:

$$S(f;x) = f_i(1-t)^2(1+2t) + f_{i+1}t^2(3-2t) + f_i' h_i t(1-t)^2 - f_{i+1}' h_i t^2(1-t), \quad (26)$$

where $h_i = x_{i+1} - x_i, t = (x - x_i)h_i^{-1}, x \in [x_i, x_{i+1}], i = 0,1,2,...,N-1$.

These splines are used for interpolation of sufficiently smoothed functions $f(x)$, given on some points of interpolation $\Delta_N : a = x_0 < x_1 < ... < x_N = b$ in fulfillment following conditions:

a) the power $S(f;x) \le 3, x \in [x_i, x_{i+1}]$;

b) $S(f;x) \in C^2[a,b]$;

c) $S(x_i) = f(x_i), i = 0,1,2,...,N; N \ge 2$ with the different kind of boundary conditions.

To find unknowns $f_i'$ and $f_{i+1}'$, the condition of continuous second derivatives at points of interpolation should be used. Both these conditions and boundary conditions allow to obtain the system of $N+1$ equations for determination of $N+1$ unknowns $f_i', i = 0,1,2,...,N$. It is well known, the matrix of this system is the nonsingular matrix with a diagonal predominance, i.e. unknowns $f_i'$ are defined identically. Different variants of the cubic spline construction have been investigated in the extensive bibliography [9,10].

Since the spline (26) is the polynomial of the power no higher than three, eq.(25) will be fulfilled exactly for $S(f;x)$ in $n \le 3$. Therefore, this spline can be represented as decomposition by functions $d_1, d_2$ and by the cubic polynomial $S_3(\tau;\lambda,L)$, provided that the single additional point between adjacent points of interpolation will be given. In this case we obtain *the new model* of the cubic spline, which uses *three* points and is equivalent for the two-point spline (26). We will call this model *the three-point model* of the cubic spline or $TPS$. As the $TPS$ model depends on the single free parameter $(\alpha = \alpha(f_i', f_{i+1}', f_i, f_{i+1}, h_i))$, then it has the important advantage with respect to the model (26) (see below).

Further, examples of algorithms based on the $\mathcal{DPT}$ approach for functions approximation, interpolation and fitting are discussed.

### *4.1 Local function approximation by the cubic parabola*

Cubic splines play the key role in the function approximation. The theory and application of cubic splines are widely covered in the extensive literature [8-11]. We shall consider the peculiarity of $\mathcal{DPT}$ for the cubic parabola on the local segment:

$$y(x) = \alpha x^3 + \beta x^2 + \gamma x + \delta, \ \alpha \ne 0, \ x \in [a,b]. \quad (27)$$

Let us fix the mark $\mathcal{R}$ on this curve at points $(x_\lambda, y_\lambda)$, $(x_0, y_0)$, $(x_L, y_L)$. By using



eq.(4) and $p_i(\tau;\lambda,L), i = 1,2,3$, we obtain:

$$y^*(x;\mathcal{R}) = h(\tau) = \alpha\lambda L\tau + y_0.$$

Shift the origin at the basis point $(x_0, y_0)$, the last expression reduces to the following form:

$$h(\tau) = \mathcal{D}[\alpha x^3 + ...;\mathcal{R}] = \alpha\lambda L\tau. \quad (28)$$

We see that the $\mathcal{D}$–transform converts the cubic parabola into the straight line with the slope $\alpha\lambda L$, and vice versa, the inverse transformation of (28) with the same mark $\mathcal{R}$ yields the original cubic curve. In accord (24), (28) and table 1 the equation of the cubic curve is written in the parametric form:

$$g(\tau;\lambda,L) = \frac{-g(\lambda)}{\lambda H}\tau(\tau - L) + \frac{g(L)}{LH}\tau(\tau - \lambda) + \alpha\tau(\tau - \lambda)(\tau - L), \quad (29)$$

where $H = L - \lambda$. In contrast to formulae (26) and (27), eq. (29) contains only the one *free parameter* $\alpha$ (the coefficient in $x^3$). To determine this parameter, we use the summation (13) and (14), taking into account $h(\lambda) = \alpha\lambda^2 L$ and $h(L) = \alpha\lambda L^2$ from (28):

$$\alpha = \frac{1}{H^2}[g'(L) + g'(\lambda) - \frac{2}{H}(g(L) - g(\lambda))]. \quad (30)$$

Up to the constant, the formula (29) presents *the three-point model* of the cubic spline ($TPS$) on the segment $[\lambda, L]$. The pivot coordinates are fixed parameters of this model and $\alpha$ is the free parameter defined by (30).

As indicated on fig.8 the $TPS$–model has the visual geometric construction.

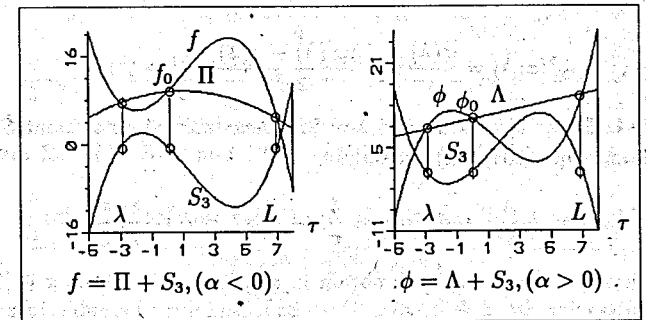


Fig.8. The geometric sense of the $TPS$–model.

The pivot coordinates are singled out on the graph. Arbitrary cubic curves $f$ and $\varphi$ are obtained as the algebraic sum of the cubic monospline $S_3(\tau;\lambda,L;\alpha)$ and the quadratic parabola $\Pi(\tau;\lambda,L)$ or the straight line $\Lambda(\tau;\lambda,L)$, depending on the location of the pivot points on the plane. Now we shall show examples of using eqs. (29) and (30) for the function approximation.

Task T1: Among curves (29), having three pivot points, a curve $g^*(\tau;\lambda,L)$ should be found, which satisfies following conditions

$$\frac{d^k\varphi(\tau)}{d\tau^k}\Big|_{\tau=\lambda,L} = \frac{d^k g^*(\tau;\lambda,L)}{d\tau^k}\Big|_{\tau=\lambda,L}, k = 0,1. \quad (31)$$

and is the approximant for the given function $\varphi(\tau) \in C[\lambda, L]$.

Usually, these conditions are used for deriving cubic splines. If derivative values $\varphi'(\cdot)$ at boundary points are known and the mark $\mathcal{R}$ on the curve $\varphi(x)$ is given, then the solution of the task (T1) is given by formulae (29) and (30).

Without loss of generality, let us consider the symmetric case in the choice of the segment borders ($a = -\lambda, b = \lambda$), $x_0 = 0$ and $\varphi(0) = 0$. To obtain the equation of the approximant, we must substitute these values into (29):

$$g^*(x;\lambda) = (2\lambda)^{-2}[\varphi(-\lambda)x(x-\lambda) + \varphi(\lambda)x(x+\lambda)] + \alpha x(x^2-\lambda^2),$$

where

$$\alpha = \frac{1}{4\lambda^2}[\varphi'(-\lambda) + \varphi'(\lambda) - \frac{1}{\lambda}(\varphi(\lambda) - \varphi(-\lambda))].$$

If $\varphi(-\lambda) = -\varphi(\lambda)$, then the equation of the cubic curve is simplified:

$$g^*(x;\lambda) = \frac{\varphi(\lambda)}{\lambda}x + \alpha x(x^2-\lambda^2), \tag{32}$$

where the parameter $\alpha$ is found by means of (30):

$$\alpha = \frac{\lambda\varphi'(\lambda) - \varphi(\lambda)}{2\lambda^3}. \tag{33}$$

Thus, the solution for (T1) is given by formulae (29) and (30). Equalities (32) and (33) present the solution of the same task for the symmetric odd function $\varphi(x) \in C[-\lambda, \lambda]$:

$$g^*(x;\lambda) = \frac{\varphi(\lambda)}{\lambda}x + \frac{\lambda\varphi'(\lambda) - \varphi(\lambda)}{2\lambda^3}x(x^2-\lambda^2). \tag{34}$$

Example 1. Let $\varphi(x) = Sinx$ and $\lambda = \frac{\pi}{2}$. Then, taking into account $Sin\frac{\pi}{2} = 1$, $Sin'(\frac{\pi}{2}) = 0$ and eqs. (33), (34), we obtain:

$$\alpha = -\frac{4}{\pi^3}, \text{ and } Sinx \approx \frac{3}{\pi}x - \frac{4}{\pi^3}x^3, \ x \in [-\frac{\pi}{2}, \frac{\pi}{2}].$$

This result is the same, as we shall obtain in approximation $Sinx$, $x \in [0, 2\pi]$ for the five points grid: $\{0 < \frac{\pi}{2} < \pi < \frac{3\pi}{2} < 2\pi\}$ by using the cubic interpolation spline. It is seen from this example that the decision for the $TPS$ model coincides completely with the classical decision for the cubic spline.

*4.2 The mean square cubic approximation of $\varphi(x) \in \mathcal{L}_2[a,b]$*

Let $\varphi(x) \in \mathcal{L}_2[a,b]$ and let the mark $\mathcal{R} \equiv \{(0,0),(\lambda,\varphi(\lambda)),(L,\varphi(L))\}$ be given on the segment $X : [\lambda, L] \subseteq [a,b]$, $\lambda \neq L$. We will solve the next task:

Task T2: The cubic approximant $S(x;\lambda,L,\alpha)$ for the smooth function $\varphi(x)$ should be found in form of (29) provided the functional $J(x;\alpha)$ achieves the minimum:

$$\min_{\alpha} J(x;\alpha) = \min_{\alpha} \int_X [\varphi(x) - S(x;\lambda,L,\alpha)]^2 dx. \tag{35}$$



The necessary condition of the minimum

$$\frac{\partial J(x;\alpha)}{\partial \alpha} = 0, \text{ where } \frac{\partial S}{\partial \alpha} = \lambda L x d_3(x;\lambda,L),$$

allows to find the required solution, i.e. to derive the parameter $\alpha$:

$$\alpha(\lambda,L) = \frac{1}{C(\lambda,L)}[\int_X x(x-\lambda)(x-L)\varphi(x)dx + \frac{\varphi(\lambda)}{\lambda H}A(\lambda,L) - \frac{\varphi(L)}{LH}B(\lambda,L)]. \tag{36}$$

Values $A, B, C$ are determined by formulae:

$$A(\lambda,L) = \int_X x^2(x-\lambda)(x-L)^2dx = \sum_{k=1}^{4} a_k(\lambda,L)(L^{k+2} - \lambda^{k+2}),$$

$$B(\lambda,L) = \int_X x^2(x-\lambda)^2(x-L)dx = \sum_{k=1}^{4} b_k(\lambda,L)(L^{k+2} - \lambda^{k+2}),$$

$$C(\lambda,L) = \int_X x^2(x-\lambda)^2(x-L)^2dx = \sum_{k=1}^{5} c_k(\lambda,L)(L^{k+2} - \lambda^{k+2}),$$

where coefficients $a_k, b_k, c_k$ are expressed via $\lambda, L$:

$$a_1 = -\frac{\lambda L^2}{3},\ a_2 = \frac{L^2+2\lambda L}{4},\ a_3 = -\frac{2L+\lambda}{5},\ a_4 = \frac{1}{6},$$

$$b_1 = -\frac{L\lambda^2}{3},\ b_2 = \frac{\lambda^2+2\lambda L}{4},\ b_3 = -\frac{2\lambda+L}{5},\ b_4 = \frac{1}{6},$$

$$c_1 = \frac{\lambda^2 L^2}{3}, c_2 = -\frac{\lambda L(L+\lambda)}{2}, c_3 = \frac{\lambda^2+4\lambda L+L^2}{5}, c_4 = -\frac{(L+\lambda)}{3}, c_5 = \frac{1}{7}.$$

If we take symmetric borders of the segment, then terms with even powers of $\lambda$ disappear for $A(\lambda)$, $B(\lambda)$ and $C(\lambda)$. In this case eq. (36) has the form:

$$\alpha = \frac{\int_{-\lambda}^{\lambda}(x^3 - \lambda^2 x)\varphi(x)dx - (a_1\lambda + a_3\lambda^3)\varphi(-\lambda) - (b_1\lambda + b_3\lambda^3)\varphi(\lambda)}{2(c_1\lambda^3 + c_3\lambda^5 + c_5\lambda^7)}. \tag{37}$$

Example 2. Again we consider the function $\varphi(x) = Sinx$, $x \in [-\lambda, \lambda]$. The cubic curve $S(x;\lambda,\alpha)$ should be found, which approximates $Sinx$ in the metric $\mathcal{L}_2$ (the criterion (35)). Using eq.(37), we obtain:

$$\alpha(\lambda) = \frac{105}{4\lambda^7}[(\lambda-3)Sin\lambda + 3\lambda Cos\lambda].$$

Taking into account that $Sin(-x) = -Sinx$ and eq.(29) we have:

$$Sinx \approx S(x;\lambda) = \alpha(\lambda)x(x^2-\lambda^2)). \tag{38}$$

If we set $\lambda = \pi$ in the expression for $\alpha(\lambda)$, we find:

$$\alpha(\pi) = -\frac{315}{4\pi^6}.$$

Substituting this $\alpha(\pi)$ into eq.(38), we obtain the following solution:

$$Sinx \approx -\frac{315}{4\pi^6}x(x^2-\pi^2).$$

Plots of $Sinx, S(x;\pi)$, $\varepsilon(x) = Sinx - S(x;\pi,\alpha)$ and $\alpha(\lambda), \lambda \in [0.1,\pi]$ are shown on fig.9.

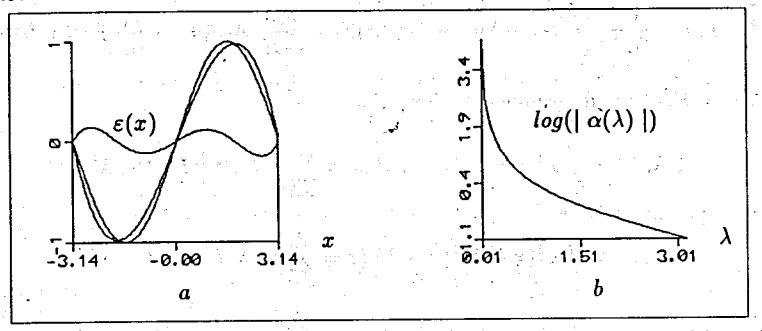


Fig.9. $Sinx, S(x;\pi)$, the error $\varepsilon(x)$ (a) and the parameter $\alpha(\lambda)$ $(b)$.

The graph shows the uniformly character of the error approximation on the whole of the interval.

*4.3 Approximation of $\varphi(x) \in C^{(n)}[\lambda, L]$ in the $\{S_n(x;\lambda,L)\}$ basis*

The eq.(25) and conditions (31) for $k = 1,2,3,...$ allow to derive the decomposition of the function $f(x) - f(0) = \varphi(x) \in C^{(n)}[\lambda, L]$ via the parameterized basis $\{S_n(x;\lambda,L)\}$ (eqs. (23), (23a)). In this case it is necessary to solve the system of equations (31) for finding parameters $\alpha_k, k = 1,2,3,....$ It follows from (23) and (25) that starting from $k = 3$, $kth$ derivatives of basis functions $\{S_k\}$ and $\{x^k\}$ coincide, whereas $kth$ derivatives of functions $d_1$ and $d_2$ are equal to zero.

Applying this scheme to approximation of the smooth function $\varphi(x)$ on the segment $[-\lambda,\lambda]$, for $x_0 = 0$, we obtain coefficients $\alpha_k$, depending on $\varphi^{(k)}(x_\mu)$, $d_1^{(k)}(x_\mu), d_2^{(k)}(x_\mu)$ and $S_{j+2}^{(k)}(x_\mu)$, where $x_\mu \in [-\lambda,\lambda]$, $\mu = 1,2; k = 1,2,...,n/2$. Matrix elements $S_{j+2}^{(k)}(x_\mu)$ can be expressed trough indices of the power $(j+2)$ and the derivative order $(k)$ as the following:

$$S_{j+2}^{(k)}(x_\mu) = \prod_{\nu=0}^{k-1}(j+2-\nu-m_{kj})x_\mu^{j+2-k}, k = 1,2,...,n/2; j = 1,2,...,n, \qquad (39)$$

where

$$m_{kj} = \begin{cases} (2-k)+k\delta(j), & k = 1,2, \\ 0, & k = 3,4,...,n/2 \end{cases}$$

and $\delta(j) = [1+(-1)^j]/2$. Indices $k$ and $\mu$ depend on the row of matrix index $i$:

$$k \equiv k(i) = [i+\delta(i-1)]/2, \quad \mu \equiv \mu(i) = 1+\delta(i), i = 1,2,...,n.$$

Example 3. Using the $9th$ power polynomial of $S_n(x,\lambda)$, find the approximation of $Sinx, x \in [-\pi,\pi]$.



Solution. Taking into account that $Sinx$ is odd function equal to zero at points $-\pi, \pi, 0$ and using eqs. (22), (25), (39) in $n = 9$, we obtain:

$$Sinx \approx 0+0+0+\sum_{j=1}^{4}\alpha_j S_{2j+1}(x;\pi).$$

Coefficients $\alpha_j$ are found as solution of eqs.(31) in $k = 1,2,3,4$. As the result the approximation of the sine has the following form:

$$\begin{aligned} Sinx \approx\ & -0.16579347(x^3 - x\pi^2) + 0.00815272(x^5 - x\pi^4) - \\ & 0.00017948(x^7 - x\pi^6) + 0.00000173(x^9 - x\pi^8). \end{aligned} \qquad (40)$$

The quality of the approximation of $Sinx$, $x \in [-\pi,\pi]$ by the $\mathcal{DPT}$-method and by the truncated Taylor-series for $n = 9$ is shown on fig.10.

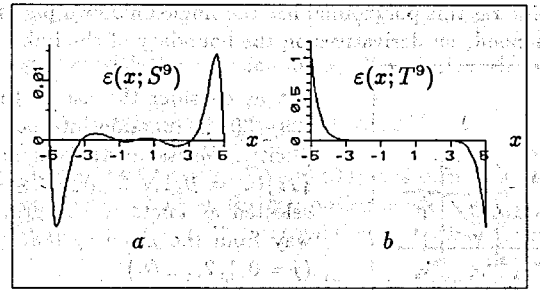


Fig.10. The errors behaviour for $S^9(x;\pi)$ $(a)$ and $T^9(x)$ $(b)$.

It is obvious, the error of approximation for (40) has the uniform behaviour.

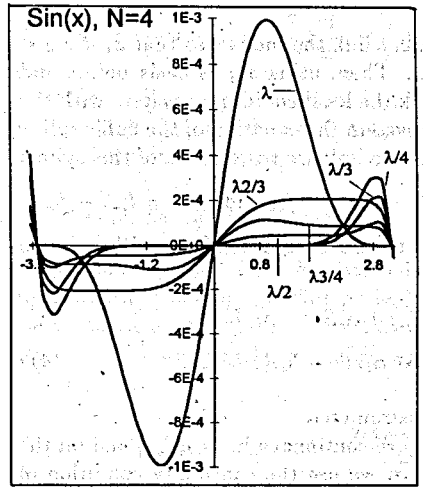


Fig.11. The error dependence of the choice of the point for $Sin'(\cdot)$.

This error is smaller almost by two orders in the some region out of the segment $[-\pi,\pi]$ than the Taylor expansion error, and yet it concedes appreciably to the latter at the center of the segment.
The experimental study of the error for $Sinx$ approximation by the use of $S_n(x;\lambda)$, $x \in [-\lambda,\lambda]$ has been carried out, using the MAPLE program, designed by C. Tőrők (TUK, Slovakia). As indicated in fig.11, the value and the shape of the error $Sinx - S_{2N+1}(x;\lambda)$ for $N = 4, \lambda = \pi$ essentially depend upon what points $(x_\mu)$ for computing of the derivative in eq.(31) are picked out. We can see that the behaviour of the error is best one for $x_\mu = \pm\frac{\lambda}{2}$.

*4.4 Interpolation by cubic splines (the TPS-model)*

Now we consider the use of the $TPS$-model in an interpolation. Let values of the sufficiently smooth function $f_k = f(x_k), k = 0,1,2,...,n$ be given on the grid $\Delta_n : a = x_0 < x_1 < x_2 < ... < x_n = b$.

It is required to construct the cubic spline, which interpolates the function $f(x)$ in points $x \in [x_k, x_{k+1}]$. It is known the solution of this task is obtained by using of the spline-interpolation [8,9]. We still found the solution on the base of the $TPS$-model, which uses the single intermediate point in the $kth$ link.

The model (29) is an algebraic equivalent to the model (26). Really, if to assume that the cubic spline $S(f;x)$ is known on the $kth$ link, i.e. $f'_k$ and $f'_{k+1}$ are founded, then the value $S(f;x_{0k})$ for the arbitrary point $x_{0k} \in [x_k, x_{k+1}]$ and eqs.(29), (30) allow identically to construct the polynomial of the power no higher than three and coinciding with the cubic spline (26) at every points $x \in [x_k, x_{k+1}]$. Due to the intermediate point $x_{0k}$ this polynomial has the single unknown parameter $\alpha$, which in accord (30) depends on derivatives on the boundary of the link.

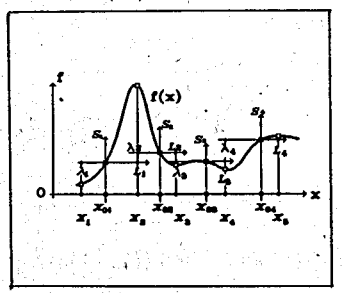


Let us consider the use of the $TPS$-model (29)-(30) in function interpolation more explicitly. We assume the odd number of points $\{x_k\}(k = 0,1,2,...,N; N \leq N_j)$ has been selected as knots of the grid in a suitable way from the given system of points $\{x_j\}$, $(j = 0,1,2,...,N_j)$.

Fig.12. The scetch of spline-interpolation for $TPS-$model.

We reindex grid points and ascribe to every link the index $i$ so that $x_i < x_{0i} < x_{i+1}, i = 1,2,...,N_i$, where $N_i = (N-1)/2$. Then, using $x_{0i}$ as basis points and the shift operation, we construct in every link the local coordinate system with the origin at the point $(x_{0i}, f_{0i})$ (fig.12). In this system the equation of the cubic spline has the form of (29) and boundary points of the link are parameters of this spline:

$$\lambda_i = x_i - x_{0i}, L_i = x_{i+1} - x_{0i}, H_i = L_i - \lambda_i, \varphi_i = f_i - f_{0i} \text{ and } \varphi_{i+1} = f_{i+1} - f_{0i}.$$

After that for $\tau = x - x_{0i}$ and $x \in [x_i, x_{i+1}]$ the $TPS$ equation in the $ith$ link will be written as

$$S_i(\tau;\lambda_i,L_i) = \Pi_i(\tau;\lambda_i,L_i) + \alpha_i S_{3i}(\tau;\lambda_i,L_i) = \frac{-\varphi_i}{\lambda_i H_i}\tau(\tau - L_i) + \frac{\varphi_{i+1}}{L_i H_i}\tau(\tau - \lambda_i) + \alpha_i \tau(\tau - \lambda_i)(\tau - L_i), \quad (41)$$

where $\tau \in [\lambda_i, L_{i+1}]$ and $\alpha_i$ is the unknown parameter.

This cubic spline and his first derivative are continuous in $[x_i, x_{i+1}]$ and on the whole segment $[a,b]$. For determination of $\alpha_i$ we use the continuity condition of the second derivative of the spline at the joining point, i.e.

$$S''_i(L_i;\lambda_i,L_i) = S''_{i+1}(\lambda_{i+1};\lambda_{i+1},L_{i+1}).$$



By fulfilling these conditions at points $x_{i+1}$ for the spline (41), we obtain the system of $N_i - 1$ equations for determination of $N_i$ unknowns in the form:

$$\mu_i\alpha_i - \mu_{i+1}\alpha_{i+1} = q_i, i = 1,2,...,N_i - 1, \quad (42)$$

where $\mu_i = L_i + H_i$, $\mu_{i+1} = \lambda_{i+1} - H_{i+1}$, $q_i = (\beta_{i+1} - \beta_i)/2$, $N_i = (N-1)/2$,

$$\beta_i = \frac{2}{\lambda_i L_i H_i}(\lambda_i\varphi_i - L_i\varphi_{i-1}) \text{ and } \beta_{i+1} = \frac{2}{\lambda_{i+1}L_{i+1}H_{i+1}}(\lambda_{i+1}\varphi_{i+1} - L_{i+1}\varphi_i).$$

For unambiguous definition of $\alpha_i$ it is necessary to add another equation. This equation one can obtain, if only the single boundary condition is given, for instance $S'_1(\lambda_1;\lambda_1,L_1) = \varphi'(\lambda_1)$. This condition allows to find the parameter $\alpha_1$ in the form

$$\alpha_1 = \frac{1}{\lambda_1^2 - \lambda_1 L_1}(\varphi'_1 - \Pi'_1), \text{ where } \Pi'_1 = -\frac{\varphi_1}{\lambda_1 H_1}(2\lambda_1 - L_1) + \frac{\varphi_2}{L_1 H_1}\lambda_1.$$

Equations (42) together with the equation for $\alpha_1$ allow to find all parameters $\alpha_i$ as follows

$$\alpha_{i+1} = \frac{\mu_i}{\mu_{i+1}}\alpha_i - \frac{q_i}{\mu_{i+1}}, i = 1,2,...,N_i - 1.$$

Under the comparison of two models (26) and (29) it is seen that the last model is significantly economic, first of all, in the computing aspect.

Example 4. We consider the $TPS$-interpolation of $f(x) = Sinx$ for the seven-points grid

$$\Delta_7 : -\frac{\pi}{2} < 0 < \frac{\pi}{2} < \pi < \frac{3\pi}{2} < 2\pi < \frac{5\pi}{2}.$$

As basis points we take $0, \pi$ и $2\pi$. Then $\lambda_i = -\frac{\pi}{2}$, $L_i = \frac{\pi}{2}$ and $H_i = \pi$ for $i = 1,2,3$. Let us use these data for calculation of $\alpha_1$:

$$\alpha_1 = \frac{2}{\pi^2}(0 - \Pi'_1) = \frac{2}{\pi^2}(\frac{2}{\pi^2}(-\frac{3\pi}{2}) - \frac{2}{\pi^2}(-\frac{\pi}{2})) = \frac{2}{\pi^2}(-\frac{3}{\pi} + \frac{1}{\pi}) = -\frac{4}{\pi^3}.$$

Values $\mu_i = \frac{3\pi}{2}, \mu_{i+1} = -\frac{3\pi}{2}, \beta_i = \beta_{i+1} = 0$ i.e. $q_i = 0$. Substituting the data into (42), we find $\alpha_{i+1} = -\alpha_i, i = 1,2,3$, which allow to obtain the terminal-decision on the every link of the segment.

*4.5 Local fitting of the cubic curve*

Possibilities of the $\mathcal{DPT}$ for fitting experimental data were shown in solving the track finding problem [2]. This problem is an urgent issue in pattern recognition and in particle physics. To solve this issue, the algorithm of adaptive projective filters ($APF$) was developed. This algorithm is based on the $LQ$-model of the track-segment:

$$y(x) = \frac{-y(x_0+\lambda)}{\lambda H}x(x-L) + \frac{y(x_0+L)}{LH}x(x-\lambda) + \frac{y(x_0)}{\lambda L}(x-\lambda)(x-L), \quad (43)$$

where $H = L - \lambda$. The $APF$-algorithm can be extended also for complex form curves tracking, for example, in contours processing [3].

We consider the use of 4-point transforms and the $TPS$-model (29) for smoothing of dispersed points. This approach allows to increase the processing speed, which is the actual problem for adaptive signal digitization, for modern data processing systems and so on [4].

The $TPS$-model of the cubic curve can be used as *the flexible structural element* for the development of adaptive algorithms in several fields of applications. Three parameters of this model are selected from input data with the accuracy of the measurement error, which no affect on the visible distortions of the contour, for the suitable choice of the value $H = L - \lambda$. Thus, the $TPS$-model has only the single free parameter $\alpha$. These properties allow to reduce several times the number of arithmetical operations under conservation of the admissible accuracy, hence, to increase the speed of computations. We consider the standard fitting process for the cubic model.

Task T3. On the given segment let us find the cubic parabola, describing the relation between measurement coordinates in the best way

$$\{x_j\} \text{ and } \{\tilde{f}_j\}, j = 1, 2, ..., N; N \gg 3,$$

where $\tilde{f}_j = f_j + e_j$, $e_j \sim \mathcal{N}(0, \sigma)$, and $x_j$ are measured without errors.

The classical decision of this task for the model (27) is obtained by using a least squares fitting ($LSF$). Estimates of four parameters are found as a result of the decision. Using eq. (25), we obtain the adequate decision of T3 for the model (29) from the condition

$$\sum_{j=1}^{N} \{\tilde{\varphi}_j - \tilde{\varphi}(\lambda) d_{1j} - \tilde{\varphi}(L) d_{2j} - \alpha \lambda L \tau_j d_{3j}\}^2 \to min$$

in the form of LSF-estimate of the parameter $\alpha$:

$$\hat{\alpha} = (\lambda L \sum_{j=1}^{N} z_j^2)^{-1} (\sum_{j=1}^{N} \tilde{\varphi}_j z_j - \tilde{\varphi}_\lambda \sum_{j=1}^{N} z_j d_{1j} - \tilde{\varphi}_L \sum_{j=1}^{N} z_j d_{2j}), \qquad (44)$$

where $z_j = \tau_j d_{3j} = \tau_j d_3(\tau_j; \lambda, L)$. Values $\tau_j$ and $\tilde{\varphi}_j$ are obtained in the shift of the origin into the basis point $(x_0, \tilde{f}_0)$ with the simultaneous change of errors $\epsilon_j = e_j - e_0$. Parameters $\lambda$ and $L$ are determined through coordinates $x_0, x_\lambda, x_L \in \{x_j\}$ so that $x_\lambda < x_0 < x_L$. Coordinates $x_\lambda$ and $x_L$ are taken on borders of the segment.

Thus, the estimate of the parameter (44) gives the decision of the task T3 for the $TPS$-model (29) in the form of $\hat{f}(x) = \tilde{f}_0 + \hat{\varphi}(x - x_0)$, where

$$\hat{\varphi}(x - x_0) = \hat{\varphi}(\tau) = \tilde{\varphi}(\lambda) d_1(\tau; \lambda, L) + \tilde{\varphi}(L) d_2(\tau; \lambda, L) + \hat{\alpha} \lambda L \tau d_3(\tau; \lambda, L). \qquad (45)$$

It is seen from eqs. (44) and (45) that the number of arithmetical operations in the model (29) is significantly less than in the case of the model (27). Furthermore, tabulation of seven functions $d_1, d_2, d_3, zd_1, zd_2, z$ and $z^2$ at points of interpolation $\tau_j \in [\lambda, L]$ reduces in addition the number of dynamically operations. The estimate has shown that even if functions $x_j^m, (m = 1 \div 6)$ are tabulated, the number of dynamically operations for the model (27) is 3-4 times greater than in the case of the $TPS$-model.



Another decision of the task T3 one can obtain by using $\mathcal{DPT}$-properties to reduce the power of the polynomial by two and to damp measurement errors. In this case the $LSF$-estimate of the parameter $\alpha$ is found from the condition

$$\min_{\alpha} \mathcal{H}(\tau_i; \alpha) = \min_{\alpha} \sum_{i=1}^{N_k} (\tilde{h}_i - \alpha \lambda L \tau_i)^2$$

in the following form

$$\hat{\alpha} = (\lambda L \sum_{i=1}^{N_k} \tau_i^2)^{-1} \sum_{i=1}^{N_k} \tau_i \tilde{h}_i, \qquad (46)$$

where

$$\tilde{h}_i = \tilde{\varphi}_\lambda p_1(\tau_i; \lambda, L) + \tilde{\varphi}_L p_2(\tau_i; \lambda, L) + \tilde{\varphi}_i p_3(\tau_i; \lambda, L), N_k \le N, (N \gg 3). \qquad (47)$$

Here the index $i$ is related to the points for which $\mid \tau_i - \lambda \mid \le T_n$ and $\mid \tau_i - L \mid \le T_n$, where $T_n$ is the threshold of the range for the "noisy" zone (see (17) and fig.5). In this connection the cubic model of input data is converted into the straight line model for almost all mapped points with the exception of, maybe, those having hit in the unstable zone (fig.5). After that the task dimension reduces by two. The using of formulae (45)-(47) for fitting of modeling data is shown on fig.13.

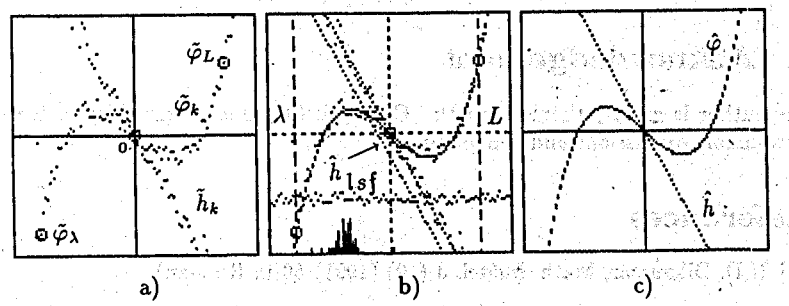


Fig.13. Fitting of the cubic curve by using of $LSF$ and $\mathcal{DPT}$ methods.

The set of points of the cubic parabola $\{\tilde{\varphi}_j\}$ are given on the grid of $100 \times 100$ pixels. Random errors $\{\epsilon_j\}$, having normal distribution and the 10 pixel variance have been added to the ordinates of the cubic curve. Parameters of the transform have been found by coordinates of three marked points, singled out on the graph. All points $\tilde{\varphi}_k$ (except of pivot) have been mapped into points $\tilde{h}_k$ by using eq.(47). The mapped points are clustered along the straight line with the slope $\hat{\alpha}\lambda L$ (a). The $LSF$-estimate of the parameter $\hat{\alpha}$ (eq.(46)) have been found on the base of $\tilde{h}_k$ points. After that, by using the inverse transform of points $\{\tilde{h}_k\}$ (45) estimates $\hat{\varphi}_k$ of the required curve have been obtained (b and c). On fig.13 (b) the straight line is shown. This line is obtained by the $\mathcal{D}$-transform of the fit for the traditional model (27) as well. Parallelism of these straight lines indicates the agreement of results, deriving by various approaches. The histogram of mapped points $\tilde{h}_k$ is shown at the bottom of the figure.

## 5 Conclusion

New transforms (direct and inverse) based on the cross-ratio of four collinear points over the smooth curve presented by the formula or by the table have been found. Since these transformations use three cross-ratio functions and three points of the curve as pivot points, the direct operation has the stability to errors everywhere except neighborhoods of two pivot points, i.e. the error suppression is the result of the direct transformation.

The transformations possess a number of the properties, which have been used for developing new rules and methods in the smooth function parametrization. The new class of polynomials (monosplines), having a good approximation quality has been derived. The new effective approach based on monosplines has been proposed for approximation and fitting of curves. In this approach the local error has the uniformity at the interval of approximation. The three-point spline model ($TPS$) of the cubic spline is proposed. The $TPS$-model allows to reduce the number of unknown parameters in twice and to obtain the advantage in the computing aspect. Approximation and fitting of curves have been shown on a number of examples.

The above results and other peculiarities of $\mathcal{D}PT$-transforms give us a new mathematical tool and a new possibility in both practical applications and theoretical research of numerical and computational methods.

## 6 Acknowledgement

The author is greatly thankful to Dr. C. Tőrők (Technical University of Košice) for valuable discussions and collaboration.

## References

[1] N.D. Dikoussar, Math. Model. 3 (10) (1991) 50(in Russian).

[2] N.D. Dikoussar, Comput. Phys. Commun. 79 (1994) 39.

[3] R.Duda and P.Hart, Pattern Classification and Scene Analysis, Wiley, New York, 1973.

[4] M. Regler, eds., Data Analysis Techniques for High-Energy Pysics Experiments (Cambridge University Press, Cambridge, 1990.)

[5] F. Klein, Vorlesungen Über Höhere Geometrie (Springer, Berlin, 1926).

[6] C. Lanczos, Applied Analysis(Prentice-Hall, 1956).

[7] G.E. Forsite, M. A. Malcom and C.B. Moler, Computer Methods for Mathematical Computations(Prentice Hall, 1977).
H. Wind, Function Parametrization. - CERN, 72-21.

[8] J.H. Ahlberg, E.N. Nilson and J.L. Walsh, The Theory of Splines and their Applications(Academic Press, New York, 1967).



[9] Y.S. Zavjalov, B.I. Kvasov and V.L. Miroshnichenko, Methods of Spline-functions(Moscow, Nauka, 1980)(in Russian).
S.B. Stechkin and Y.N. Subbotin, Splines in Computer Mathematics(Moscow, Nauka, 1976)(in Russian).

[10] B.A. Popov, An Uniform Approximation by Splines(Kiev, Naukova Dumka, 1984)(in Russian).

[11] N.N. Kalitkin and L.V.Kusmina, Mathem. Model. 6 (4) (1994) 77(in Russian).

[12] D. Roy, R. Bhattacharya and S. Bhowmick, Comput. Phys. Commun. 78 (1993) 29.

[13] Tarek M. Nabhan, Albert Y. Zamaya, Neural Networks 7 (1) (1994) 88.

Received by Publishing Department
on April 5, 1996.